
Check for updates

terization,
as above, but at
(DI) water instead of
cid (HCl) (Daejung Chemicals
phenolphthalein (p/p) mixture (Sigma
and water 1:1) were used for acid-base ti-

Neutron measurements of structure and composition

For a survey of membranes we used all five membranes described above, non-cosslinked PBI, 5% crosslinked PBI, 10% crosslinked PBI, and the commercial membranes Dapozol and FAAM-55.

The membranes were cut with a punching tool into 14 mm diameter discs and immersed in the preheated KOH solutions for the desired amount of time, ranging from one minute to 24 h for the 50 wt% KOH solution while maintaining the temperature constant at 80 °C in an oven. For the 5 wt% and 25 wt% KOH the doping was only performed for 24 h and also at 80 °C. The vials were closed for the doping times over 10 min to prevent evaporation. After doping for the desired amount of time, the membrane discs were removed from the solution and the excess KOH was removed (by blotting) at room temperature. The weight of all samples was measured before and after the doping as a first indication of K uptake. The samples were held at room temperature in closed vials until the SANS measurements which were performed within 24 h of sample preparation.

For the SANS measurements, a Peltier-heated sample holder was used to hold the membrane samples at a temperature of 80 °C during the entire course of the experiment, which took around 24 h. Stacks of 3 membrane disks were used to increase the scattered signal intensity. The accessed momentum transfer, *i.e* Q-range from 7.5×10^{-3} to 0.43 $Å^{-1}$, was obtained with two detector distances of 2 m and 8 m and the data was calibrated to a scattering standard. The 2 m data was acquired for 5 min and the 8 m data for 1 h. Absolute scattered intensity units for the data were problematic to obtain due to thickness variations of the membranes and also different thickness swelling due to the doping. As a result, for clarity of the presented curves we scaled the data to match the incoherent background at high Q values of the sample doped at 25 wt% for 24 h. Further study would be required to extract numerical information concerning the absolute volume or density of structures in the doped samples, but for the analysis presented here this rescaling does not affect the data or the drawn general conclusions.

After performing the SANS measurements, the samples were sealed in Teflon bags and stored for the PGAA measurements which were done at a later time, after a few weeks, due to the scheduling availability of measurement time. For the PGAA measurement, since the method measures the global elemental composition, long term stability of the sample is not a concern, as the K will be contained in the sealed bag.

The PGAA measurements were conducted on the samples under vacuum with an evacuated neutron flight path to eliminate background from air. Each PGAA sample spectra is carefully corrected for the detector efficiency and the no-sample background. Stacks of 3 membrane disks as previously used for the SANS measurements were used to increase the sample volume and resulting signal intensity. Each sample was measured from 2 to 15 min to obtain very high statistics. The background was measured for 6 h to obtain the needed statistical accuracy.

PGAA, as indicated by the name, measures the unique prompt

...or all es-
...t weight of the
...of the membrane and
...olution containing KOH was
...or change from vibrant pink to col-
... n_{KOH} is simply $C_{HCl}V_{HCl}$.

...*ance and ion conductivity*

Through-plane ion conductivity of doped membranes was measured by impedance spectroscopy (ZAHNER-elektrik GmbH & Co. KG). The membranes were fixed between two chambers with an active electrode area of 1.767 cm^2. The distance between the electrodes (gold coated copper discs at the end of the chambers) was 1.59 mm. The experiment was started by filling both chambers simultaneously with 25 wt% KOH solution. The resistance of the membrane (R_m) was obtained by subtracting the resistance of the solution filled cell without membrane from the resistance obtained with membrane for 1, 5, 10, 30, 60 min and 24 h, respectively. Then the conductivity σ_m was calculated as according to Eq. (2) with membrane thickness values, t, obtained from the dimensional change measurement where A is the area of the electrode.

$$\sigma_m = \frac{t}{R_m \bullet A} \tag{2}$$

...s we
...one and are
...ng absolute K uptake
...-doping mass which would
...esidual solvent levels. Here possible
...ations of the dimethylacetamide (DMAc),
...prepare the membranes, could give systematic con-
...s to the PGAA data. Residual DMAc, since it contains N, if present in the prepared membranes would leach out slowly during the KOH doping procedure, giving an extra N contribution in the PGAA signal that would decrease over KOH doping time and as a function of doping conditions. However, measurements of residual DMAc [25] show that we can estimate that the maximum amount of additional N signal in the PGAA spectra arising from DMAc would be below a few percent of the membrane signal and insignificant compared to the trends observed and conclusions of this paper. To check the validity of this assertion, we remeasured the PGAA spectra after the samples were allowed to dry in the vacuum for one day. In this case the intensity of the N signals remained unchanged within errors. As an additional check, the K concentration was also analyzed as a function of the H concentration of the fully desiccated samples, thus using instead the H atoms of the polymer to provide the fixed reference. These data trends using H gave results proportional to the data that used N as a reference. Further the ratio of 3 H atoms per N atom observed with PGAA corresponded to the expected value for PBI typically within 4%, again supporting the assertion that the possible DMAc (ratio of 9H per N) is below a few percent.

The SANS measurements of the initial samples showed structure peaks in the data for the non-cross linked PBI samples, thus we focused on this membrane for a further study of the structure development with respect to doping conditions. These PBI membranes were prepared in the same way as described above, however this time we focused around the area of maximum K uptake, doping the PBI at concentrations of 15 wt%, 20 wt%, 25 wt%, 30 wt%, and 35 wt% each for 24 h at 80 °C. Additionally, we did a time dependence study of the membranes doped with 25 wt% KOH by measuring at the doping times of 1, 5, 10, 30, 60 min and 24 h. These samples where then measured with PGAA and SANS in the same way as described previously in this section.

2.3. Swelling measurements and composition via titration

For obtaining the swelling, *S,* during doping a membrane, a sample of 4 cm x 1 cm dimension was washed in DI water for two days with several water refreshments and dried for one day under atmospheric conditions (21 °C, 40–45%RH) before doping. The length and thickness were recorded before dopping as the dry dimensions, d_{dry}, and during the doping at 1, 5, 10, 30, 60 min and 24 h respectively giving the wet dimensions, d_{wet} in order to determine the swelling given as

3. Results and discussion

3.1. Composition determined with PGAA

The first set of neutron experiments we present used PGAA to explore the dependence of the K content in the doped membrane on the KOH concentration of the doping solution, using solutions of 5, 25 and 50 wt% KOH. For comparison, also an undoped membrane was analyzed. The results of PGAA measurements in Fig. 1 show the variation in relative K content for the series of 5 different membranes. All of the membranes shown here resulted in a maximum K uptake of about 0.4–0.5 K atoms per N in the polymer chain. Interestingly the initial uptake within the first minutes leads to an almost saturated level of K concentration except for FAAM-55 which had somewhat slower uptake kinetics. The uptake of the 25 wt% KOH solution for 24 h leads to similar doping levels for PBI and 5 wt% crosslinked PBI, and even slightly higher K content when compared to the same membranes doped with the 50 wt% KOH solution for 24 h. This might be due to osmotic pressure effects and a stronger water swelling for the 25 wt% KOH solution. Incidentally, these values are consistent with other work which showed an optimal uptake at around 25–35 wt% KOH concentration [8].

For the second set of samples the time dependence of the KOH doping for the non-cross-linked PBI membrane doped at 25 wt% KOH was explored by varying the doping time from 1 min to 24 h, and the KOH doping concentration was varied from 15 wt% to 30 wt% in 5 wt% steps for a fixed doping time of 24 h. The results of the PGAA measurements on this series of samples are shown in Fig. 2A and B. As shown in Fig. 2B, the relative K content reaches a maximum at 20–25 wt% KOH doping concentration as in the prior measurement, and Fig. 2A shows the K content has reached ca. 90% of the 24 h uptake value after only 1 min and is thus nearly independent of the time it was doped.

…btained …data in Fig. 3A …uptake of K, the nano- …o evolve in the membrane on …ner, the data in Fig. 3B shows that the …r 24 h is highly dependent on the KOH doping …This dynamic structure formation gives us a com- …tary picture to the relatively static K uptake from the PGAA data.

To elucidate the structural changes, we fit the measured intensity data, *I(Q)*, to the Teubner-Strey bicontinuous model. Alkylated-PBI membranes have shown to give local lamellar structure with SAXS measurments [31] however this scattering occurs at larger Q-values, i.e. from smaller size scale structures, than the peaks observed in our data. Assuming a similar local lamellar structure in the KOH doped PBI here, the scattering by larger size scale structures suggest we are observing inter-domain channels that are being formed during the doping process. In this case of a two component structure presumably consisting of disordered domains of locally lamellar polymers and inter domain channel like structures containing the KOH solution. For such systems without a well defined particle shape, the Teubner-Strey is an often used model that can describe the relevant features of our data [26,27]. The functional form of this model plus a Porod-law and flat a background is used to fit the data. This model can be written as,

$$I(Q) = B + \frac{A}{Q^n} + \frac{C}{Q^4 - 2(Q_0 - \xi^{-2})Q^2 + (Q_0^2 + \xi^{-2})^2} \quad (3)$$

…th the Teubner-Strey portion as deduced in Ref. [28]. Here A and C are scale parameters, n is the Porod exponent, B is the background, Q_0 is the correlation peak center which is related to the domain repeat distance or d-spacing by $d = 2\pi/Q_0$ and ξ is the correlation length which is a measure of the dispersion in d[28]. In our fits n was about -4 and the background was held to a common value of 0.285 (cm^{-1}). The data was fit to an intermediate range spanning the Porod-like low Q-range to past the correlation peak.

The fits for the SANS data in Fig. 3A exploring the structure variation as a function of doping time for 25 wt% KOH doping solution are summarized in Fig. 4A and B. Fig. 4A shows that nano-structures with a repeat distance of d = 19.9 ± 0.2 nm have formed by 1 min, visible as a peak at Q~0.31 nm^{-1} that decreases at longer time scales where the peak is nearly disappearing for doping times of 1 h and 24 h. The correlation length, initially 5.6 ± 0.2 nm at 1 min, appears to slightly increase up until 10–30 min after which it decays, as further evidenced by the data in Fig. 4.B below. This implies a more ordered inter domain structure observable after initial doping decaying into a more amorphous structure as the doping progresses.

Fig. 5A and B show the fit parameters for the SANS data from Fig. 3B studying the KOH concentration dependence with 24 h doping time. Here we don't yet see a correlation peak at the lowest KOH concentration of 15 wt%, while a peak with d-spacing corresponding to a domain repeat distance of 17 ± 5 nm becomes visible at 20 wt% KOH and the d-spacing decreases with increasing KOH concentration down to 10.2 ± 0.5 nm at 35 wt% KOH. While in this data series the higher concentration maintained a significant structure peak for 24 h doping time, the d-spacing was about half the values of those for the 25 wt% doping series at low doping times, and the correlation lengths for all the

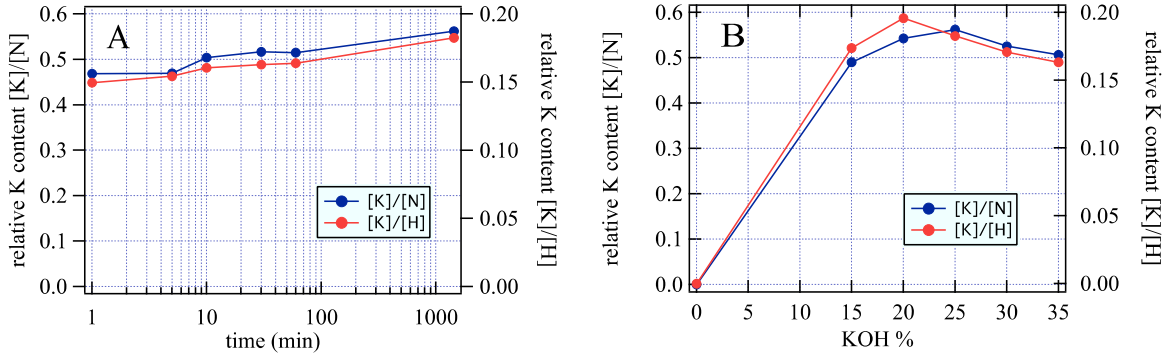

Fig. 2. Graphs showing the uptake of K in the PBI membrane as measured with PGAA relative to the N atoms in the polymer backbone (left axis open blue markers) or the H content in the desiccated sample (right axis closed red markers) (color available online). **Graph A** shows the increase in K uptake vs. time for 25 wt% KOH, **Graph B** shows the K uptake as a function of the KOH doping concentration for a 24 h doping time. The lines are to guide the eye, and the statistical errors are smaller than the marker size. Also presented are the K uptake data relative to the H concentration of the desiccated sample (red) which showed a typical −4% deviation from the N referenced data, the 20 wt% data point gave a maximum deviation of 8%. The SANS data for the samples shown in graphs A and B are given in Fig. 3A and B, respectively.

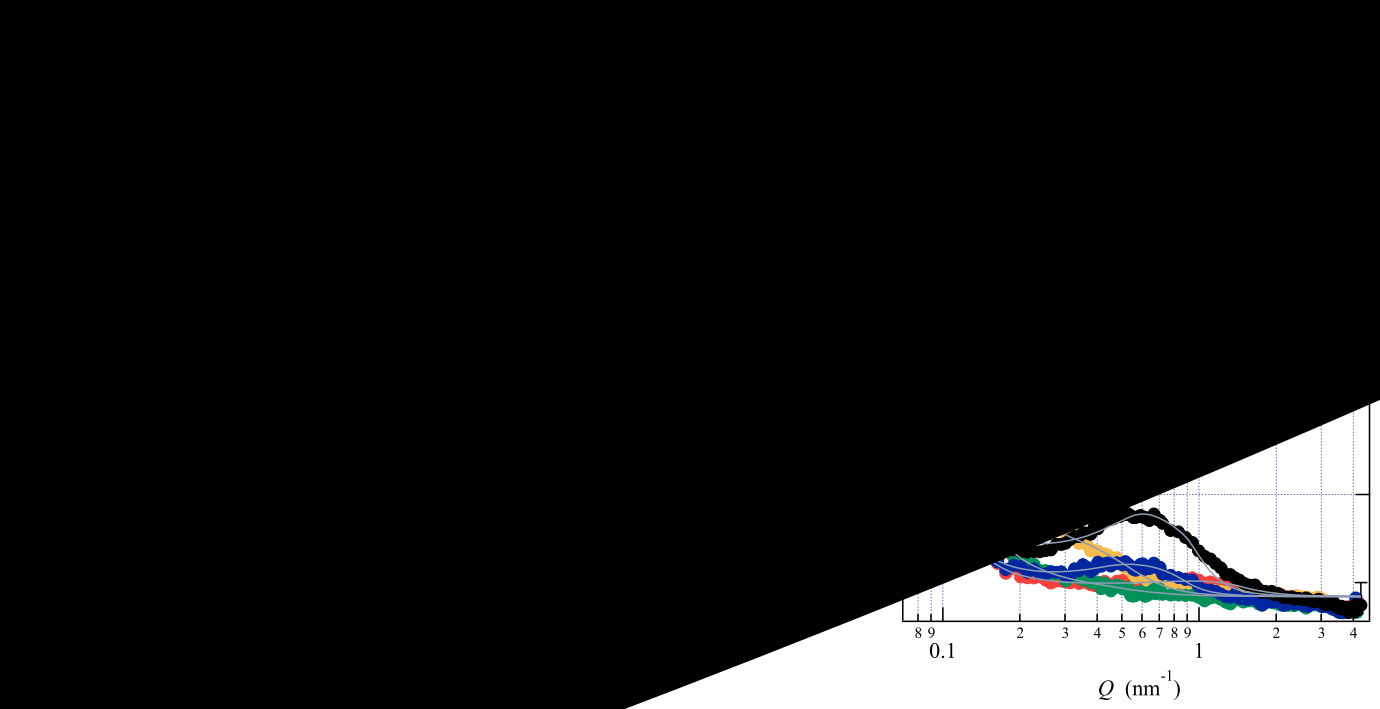

colored lines are to guide the eye, and the grey lines are the fits to the data using Eq. (2) (color available doping time using a 25 wt% KOH doping solution. The diffraction peak in the 30 min data corresponds to 16 nm sponds to 20 nm structures. The PGAA data for the samples shown in this graph are given in Fig. 2 A. **Graph B.** SANS data as a on concentration (doping time: 24 h). The strong correlation peak in the 30 wt% and 35 wt% occurs for a nano-structure size of about d 20 wt% KOH doped samples show an increased forward scattering presumably due to the formation of larger domains with increased D_2O ng. The PGAA data for the samples shown in this graph are given in Fig. 2B.

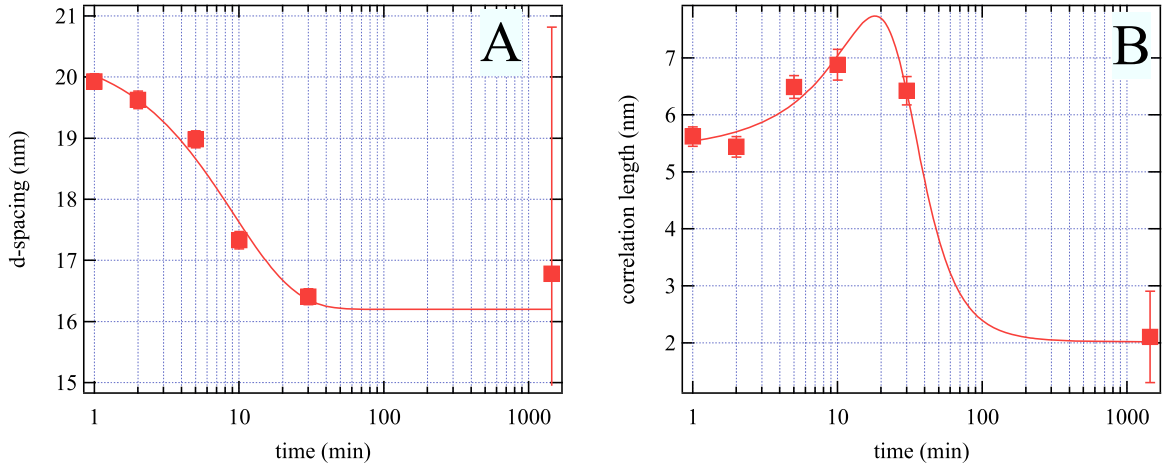

Fig. 4. Results of the fits using eq. 4 for the SANS data shown in Fig. 3A of the structure vs. time for PBI doped with 25 wt% KOH. **Graph A** shows the d-spacing of the structures in the membranes with an exponential fit line to guide the eye, the 24 h (1440 min) data point has a 40% error due to the low amplitude of the observed peak. **Graph B** shows the correlation length of the structures formed with a Lorentzian fit line only to guide the eye. Both plots are as a function of time during doping in 25 wt% KOH.

24 h doped samples were also approximately half that of the samples doped for short times (< 1 h). Again supporting the premise that the KOH initially forms ordered structures, with the KOH entering between domains in the PBI that are being broken up in time and with higher KOH concentration.

Given the variations in the SANS curves and resulting fit parameters in Figs. 4 and 5, we assume there are more variables in the process to control and a further and more detailed study could help better understand these trends. In the future we would aim to understand the variations in the relative correlation peak size to understand why the 30–35 wt% at 24 h doping time sample produced large peaks as opposed to the nearly absent peak for the 25 wt% 24 h doped samples, which for now we assume was due to variations in the samples or sample preparation. The peaking nature of the ξ-values in Fig. 4B may be fortuitous, the fit-line in the plot is only added to guide the eye, and more data points in this region would be required for conclusive information. However, due to the limited availably of neutron beam-time such additional study was not yet performed.

Extended studies covering a broader Q-range either via neutrons and/or X-rays, could be used to gain understanding of the interplay between this possible inter-domain structures discussed here and possible local lamellar structure discussed in the following section, but this was beyond the scope of the current work.

Since the time scales of both the SANS and PGAA measurements are on the order of minutes for such membranes, one can envision eventual in-situ doping studies to further elucidate the processes involved. A main conclusion of this work is that this combination of PGAA and SANS could also be useful for *in-operando* studies of functioning fuel cells and electrolysis cells as a function of conditions and cycling because of its sensitivity to changes in composition and structure.

...ture vs. KOH concentration for a 24 h doping time. **Graph A** shows the d-spacing ...gth of the structures after a doping time of 24 h for varying concentrations of KOH. The

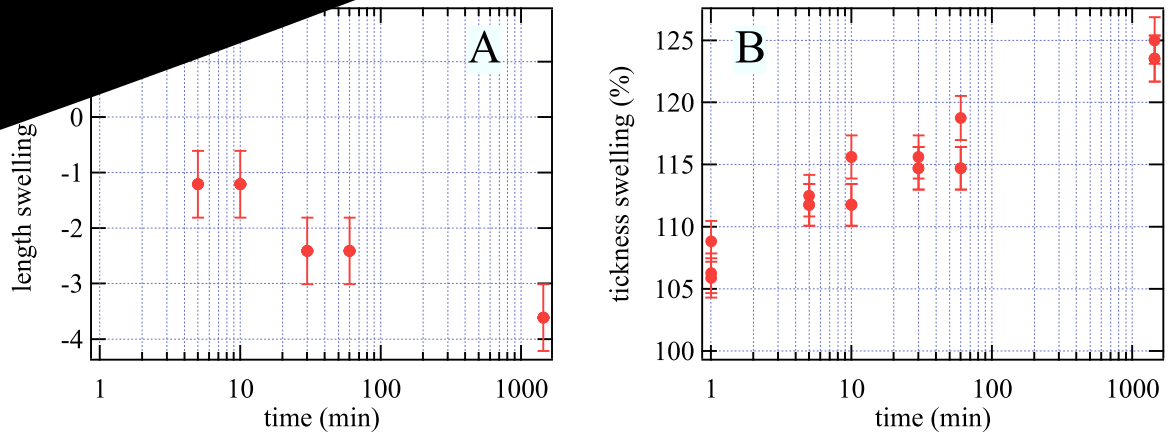

Fig. 6. Length swelling (A) and thickness swelling (B) of the membrane during 25 wt% KOH doping.

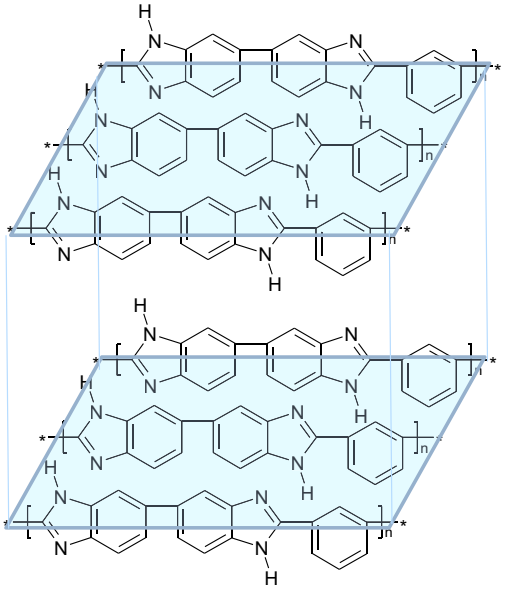

Fig. 7. An assumed lamellar structure of PBI which could explain the observed anisotropic swelling during doping.

Table 1
Composition of PBI membranes after different immersion times in 25 wt% KOH solution at room temperature.

Time	KOH uptake wt %	Water uptake wt %	Total uptake wt %	K/N ratio
1 min	39.6 ± 1.5	109.7 ± 0.2	149 ± 2	0.544 ± 0.020
1 h	39.7 ± 1.1	105.3 ± 3.9	145 ± 5	0.546 ± 0.015
1 day	39.9 ± 0.2	104.0 ± 5.3	144 ± 6	0.548 ± 0.003

3.3. Swelling and composition via titration results

When the membranes are immersed in 25 wt% KOH solution, they swell immediately in all directions, with a very strong preference towards swelling in thickness, or the z direction. After a few minutes, the membranes shrink in length, i.e the in-plane dimension x or y, while the z direction still increases. Because the z-direction swells much stronger than the x or y direction, the volume swelling follows the same trend as the thickness swelling, and continuously increases after contact with KOH solution. We paid special attention to the measurements of the in-plane, i.e. x or y, dimension swelling to insure it is isotropic in these dimensions leading one to support a local lamellar structure in these membranes as opposed to a kind of nematic structure, in which all polymer chains are oriented along the casting direction.

Fig. 6A and B show this swelling in the length and thickness, respectively. Anisotropic swelling of PBI membranes is known for

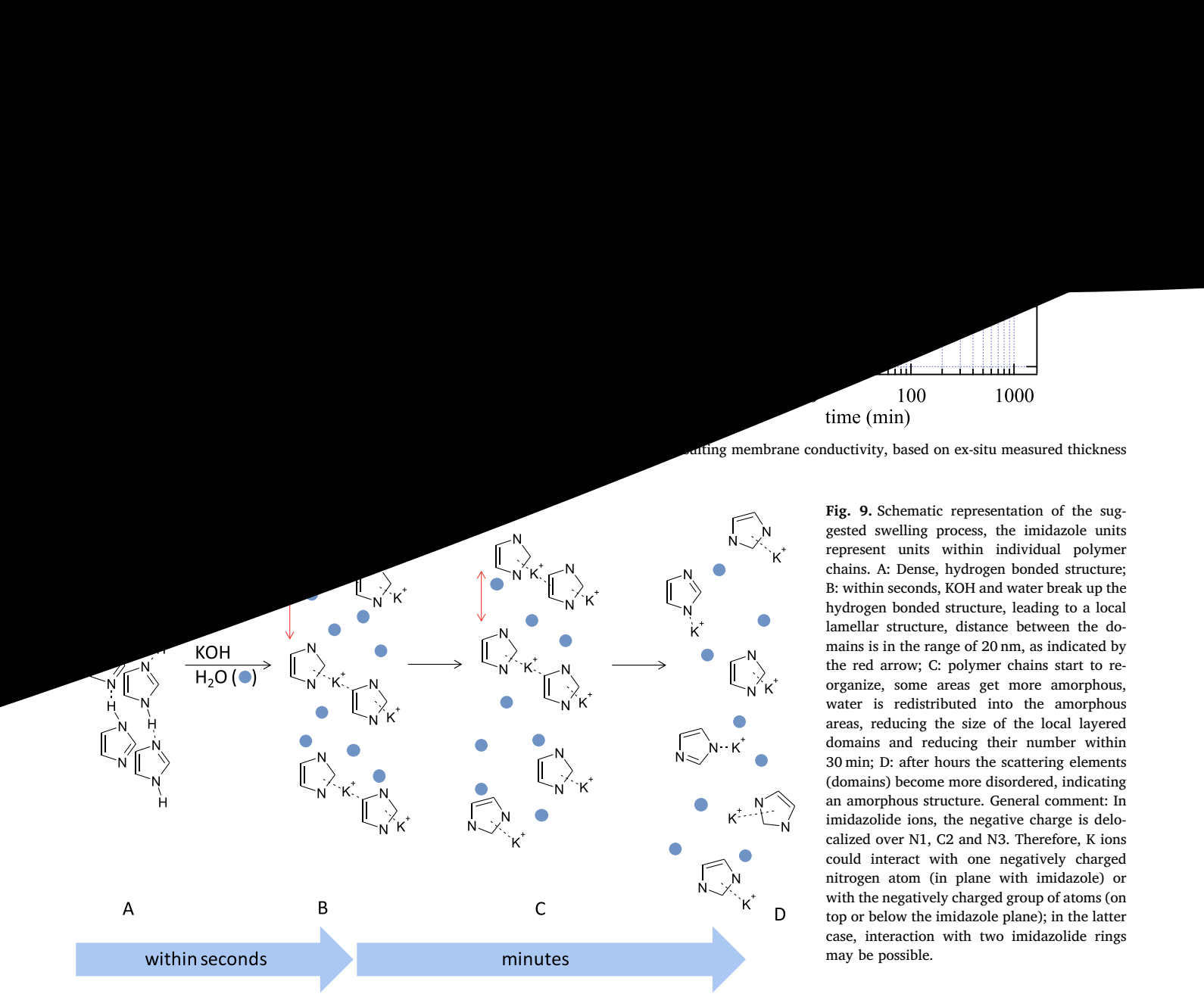

Fig. 9. Schematic representation of the suggested swelling process, the imidazole units represent units within individual polymer chains. A: Dense, hydrogen bonded structure; B: within seconds, KOH and water break up the hydrogen bonded structure, leading to a local lamellar structure, distance between the domains is in the range of 20 nm, as indicated by the red arrow; C: polymer chains start to reorganize, some areas get more amorphous, water is redistributed into the amorphous areas, reducing the size of the local layered domains and reducing their number within 30 min; D: after hours the scattering elements (domains) become more disordered, indicating an amorphous structure. General comment: In imidazolide ions, the negative charge is delocalized over N1, C2 and N3. Therefore, K ions could interact with one negatively charged nitrogen atom (in plane with imidazole) or with the negatively charged group of atoms (on top or below the imidazole plane); in the latter case, interaction with two imidazolide rings may be possible.

phosphoric acid doped membranes, although to a much lesser degree. Usually, the thickness swells 1.2–1.5 more than the x direction [29]. The reason for this anisotropic swelling behavior seems to be the arrangement of the polymer chains. WAXS data indicates two forms of interactions between the chains, parallel ring stacking (d spacing of 0.35 nm, typically observed in solution casted membranes), and staggered side-to-side packing (d spacing of 0.46 nm, typically observed for membranes prepared in the sol-gel-process) [30].

For an alkylated PBI, a phase separation into a lamellar structure was proven by SAXS [31]. Hence, at least partially, PBI chains may be packed in a similar way as described in Fig. 7. Since such local lamellar structures would be expected to be parallel to the x,y direction (parallel to the glass plate and casting direction), the observed initial swelling in the thickness direction when membranes are immersed in 25 wt% KOH solution suggests that the space between PBI local lamellar structures is filled rapidly with KOH solution. Then, on a slower time scale, the densely packed chains re-arrange. Movement in all directions leads to shrinking in the x and y direction.

As shown in Table 1, the weight gain was monitored for membranes doped for 1 min, 1 h and 24 h. Interestingly, while the volume swelling increased continuously, weight gain was constant within errors. This indicates a changed density, e.g. by less tight packing of polymer chains, supporting the suggested morphological changes during doping. The K/N ratio is practically constant, except for a very slight increase over time, in line with the data obtained by PGAA.

3.4. Resistance and ion conductivity results

The conductivity of pure PBI was reported to be in the range of about 10^{-9} mS/cm [32], whereas doping with acids or bases increases the conductivity into the range of 10^{1} - 10^{2} mS/cm. Since the composition of the membranes practically immediately reaches a K/N ratio of 0.5, a steep increase in conductivity is expected to occur within the first few seconds. After that, the increase should be minimal. However as shown in Fig. 8, the membrane through-plane resistance continuously increases over the observed time of 24 h. This supports the assumed lamellar structure (Fig. 2). Obviously, the presence of charge carriers will lead to a high conductivity, which will be further increased when the polymer chains rearrange into all directions, opening passages for ions migrating between the two membrane surfaces.

4. Conclusions and future steps

Fig. 9 proposes a conceptual understanding of the mechanisms

ger or

higher de-

ps changing over time.

o explore the doping process

more complete information on the

g doping in real time in order to help max-

ivity and durability of KOH doped polybenzimidazole

es. Additionally these neutron methods may also enable *in-operando* study of the evolution of the compositional, structural and electrochemical properties of these membranes over time during electrochemical cycling in water electrolysis systems. Further, these neutron methods could also help characterize and optimize doping parameters through the possibility of in-situ doping measurements. We have already explored in-situ measurements of nafion membranes in a humidity chamber to show that such *in-operando* and in-situ measurements would indeed be feasible for both PGAA and SANS given a suitable neutron-adapted cell, which will be presented in other publications.

Acknowledgements

DH and AK received funding from KIST institutional funding.

References

[1] W. Kreuter, H. Hofmann, Electrolysis: the important energy transformer in a world of sustainable energy, Int. J. Hydrog. Energy 23 (1998) 661.
[2] D.L. Stojic, M.P. Marceta, S.P. Sovilj, S.S. Miljanic, A. Photoelectrochemical, Model of proton exchange water electrolysis for hydrogen production, J. Power Sources 118 (2003) 315.
[3] R. Steinberger-Wilckens, W. Lehnert (Eds.), Innovation in Fuel Cell Technology, RSC Publishing, Cambridge, 2010.
[4] M. Carmo, D. Fritz, J. Mergel, D. Stolten, A comprehensive review on PEM water electrolysis, Int. J. Hydrog. Energy 38 (2013) 4901–4934.
[5] J.A. Asensio, S. Borro, P. Gomez-Romero, Polymer electrolyte fuel cells based on phosphoric acid-impregnated poly(2,5-benzimidazole) membranes, J. Electrochem. Soc. 151 (2004) A304–A310.
[6] K.A. Page, C.L. Soles, J. Runt (Eds.), Polymers for Energy Storage and Delivery: Polyelectrolytes for Batteries and Fuel Cells, ACS Symposium Series, ACS, Washington DC, 2012.

ensen, Towards
ne water electrolysis,

, M.R. Kraglund, D. Aili, J.H. Jang,
branes of polybenzimidazole and an anion
ine water electrolysis: improved alkaline stabi-
mbr. Sci. 564 (2018) 653–662.
development of proton conducting polymer membranes for
methanol fuel cells, J. Membr. Sci. 185 (2001) 29–39.
su, T.D. Gierke, Ion transport and clustering in nafion perfluorinated
membranes, J. Membr. Sci. 13 (1983) 307–326.
[15] O. Ivanova, W. Lüke, A. Majerus, M. Krutyeva, N.K. Szekely, W. Pyckhout-Hintzen, M.-S. Appavou, M. Monkenbusch, R. Zorn, W. Lehnert, O. Holderer, Influence of morphology on physical properties of poly(2,5-benzimidazole) membranes, J. Membr. Sci. 533 (2017) 342–350.
[16] G.J. Kearley, V.K. Peterson (Eds.), Neutron Applications in Materials for Energy, Springer, Cham, 2015.
[17] M. Höh*, T. Arlt, N. Kardjilov, I. Manke, J. Banhart, D.L. Fritz, J. Ehlert, W. Lüke*, W. Lehnert, In-operando neutron radiography studies of polymer electrolyte membrane water electrolyzers, ECS Trans. 69 (2015) 1135–1140.
[18] A. Radulescu, V. Pipich, H. Frielinghaus, M.-S. Appavou, KWS-2, the high intensity / wide Q-range small-angle neutron diffractometer for soft-matter and biology at FRM II, J. Phys. Conf. Ser. 351 (2012) 012026.
[19] Zs Révay, P. Kudějová, K. Kleszcz, S. Söllradl, C. Genreith, In-beam activation analysis facility at MLZ, garching, Nucl. Instrum. Methods Phys. Res. A 799 (2015) 114–123.
[20] A. Radulescu, N.K. Szekely, M.-S. Appavou, V. Pipich, T. Kohnke, V. Ossovyi, S. Staringer, G.J. Schneider, M. Amann, B. Zhang-Haagen, G. Brandl, M. Drochner, R. Engels, R. Hanslik, G.J. Kemmerling, Studying soft-matter and biological systems over a wide length-scale from nanometer and micrometer sizes at the small-angle neutron diffractometer KWS-2, J. Vis. Exp. 118 (2016) e54639.
[21] Danish Power Systems Ltd., Egeskovvej 6C, DK-3490 Kvistgård, Denmark.
[22] FUMATECH BWT GmbH, Carl-Benz-Str. 4, D-74321 Bietigheim-Bissingen.
[23] Q. Li, C. Pan, J.O. Jensen, P. Noyé, N.J. Bjerrum, Cross-linked polybenzimidazole membranes for fuel cells, Chem. Mater. 19 (2007) 350–352.
[24] G.L. Molnár, Handbook of Prompt Gamma Activation Analysis, Kluwer Academic Publishers, 2004.
[25] A. Majerus, PhD thesis, Eigenschaften des Phosphorsäure-Polybenzimidazol-Systems in Hochtemperatur-Polymerelektrolyt-Brennstoffzellen, p. 56, Reihe Energie & Umwelt, Energy & Environment, Volume 210 D 82 Diss., RWTH Aachen University, (2014) ISSN 1866-1793.
[26] M. Teubner, R. Strey, Origin of the scattering peak in Microemulsions, J. Chem. Phys. 87 (1987) 3195.
[27] J.M. Serpico, S.G. Ehrenberg, J.J. Fontanella, X. Jiao, D. Perahia, K.A. McGrady, E.H. Sanders, G.E. Kellogg, G.E. Wnek, Transport and structural studies of sulfonated styrene-ethylene copolymer membranes, Macromolecules 35 (2002) 5916–5921.
[28] M. Mihailescu, M. Monkenbusch, H. Endo, J. Allgaier, G. Gompper, J. Stellbrink, D. Richter, B. Jakobs, T. Sottmann, B. Farago, Dynamics of bicontinuous microemulsion phases with and without amphiphilic block-copolymers, J. Chem. Phys. 115 (2001) 9563.
[29] J.S. Yang, L.N. Cleemann, T. Steenberg, C. Terkelsen, L. Qingfeng, J.O. Jensen, H.A. Hjuler, N.J. Bjerrum, R.H. He, High molecular weight polybenzimidazole membranes for high temperature PEMFC, Fuel Cells 14 (2014) 7–15.
[30] K.A. Perry, PhD Thesis, Rensselaer Polytechnic Institute (Troy, NY), 12, 2009.
[31] P.H. Dominguez, K. Grygiel, J. Weber, Nanostructured poly(benzimidazole) membranes by N-alkylation, eXPRESS Polym. Lett. 8 (2014) 30–38.
[32] J.A. Asensio, E.M. Sanchez, P. Gomez-Romero, Proton-conducting membranes based on benzimidazole polymers for high-temperature PEM fuel cells. A chemical quest, Chem. Soc. Rev. 39 (2010) 3210–3239.